IEEJ TRANSACTIONS ON ELECTRICAL AND ELECTRONIC ENGINEERING
IEEJ Trans 2014; **9**(s1): S37–S43
Published online in Wiley Online Library (wileyonlinelibrary.com). DOI:10.1002/tee.22043

Paper

An Impedance Measurement of a Small-Capacitance Circuit using Transient Responses for Lightning Surge Analysis

Diah Permata[a], Student Member
Naoto Nagaoka, Member

A method to measure a small capacitance with its loss resistance using a set of transient current waveforms is proposed in this paper. The parameters are obtained from the time constants in the time domain. The method has high resistance to extraneous noise, because a time-to-frequency transformation, which is sensitive to noise, is not required. The transient current waveforms are obtained by a voltage or current source, a current transformer, and a waveform recorder. The measured capacitance by the proposed method is not affected by the capacitance of the voltage probe, because it is obtained without any voltage information. The sheath surge impedance of the current injection cable, which is indispensable for the transient measurement, is corrected. The application of the method has the advantage in that it allows the modeling of a fast transient of a power apparatus, comparing it with the steady-state measurement using an impedance measuring instrument. The proposed method is applied to create an equivalent circuit between electrodes implanted into a piece of wood, and its reliability is confirmed by comparison between the measured and calculated results. Stray capacitances of a miniature circuit breaker are also measured, and the results show that the proposed method is applicable to equipment in power systems. © 2014 Institute of Electrical Engineers of Japan. Published by John Wiley & Sons, Inc.

Keywords: small-capacitance circuit, time constant, equivalent circuit, transient analysis, sheath surge impedance, lightning surge

Received 7 March 2014; Revised 25 June 2014

1. Introduction

Transient assessment is required in the field of power engineering to verify the immunity of electrical and/or electronic equipment connected to power systems. Lightning is one of the key phenomena to be taken into account for insulation design of power systems. For the estimation of the lightning surge, stray capacitance has to be taken into account even if it is only some picofarads because the surge includes high-frequency components. An accurate measurement of the small capacitance is indispensable.

Measurement methods for small capacitance have been proposed in many fields, such as thin-film technology [1], electronic circuit [2,3], etc. These measurements have been carried out in a steady state, i.e. using a high-frequency, low-power sinusoidal source.

The authors have reported a measured result of the small capacitance of a specimen by the steady-state measurement [4]. Although the method is applicable in a laboratory test, it is difficult to apply to the field of power systems whose measuring object is larger than the electronic devices. Instability due to a radio interference is a problem when it is applied to a practical system.

The capacitance can be obtained from a set of transient voltage and current responses with a time-to-frequency transformation, such as numerical Fourier transform. The ratio between the voltage and current responses in a frequency domain gives an impedance as a function of frequency. The loss resistance and capacitance are obtained from its real and imaginary part, respectively. The numerical Fourier transform is, however, sensitive to noise and its truncation error is unavoidable [5]. The parasitic capacitance of the measuring system, i.e. a voltage probe, which is indispensable to the measurement, is also a fatal disadvantage for an estimation of the small capacitance of a specimen as the authors have been reported [5]. A precise method to measure the small capacitance is required.

We had reported a measuring method that excludes the parasitic capacitance of the voltage probe and the numerical noise due to the time-to-frequency transformation using a ramp voltage source and an electromagnetic field analysis [6,7]. The capacitance is obtained as the ratio of the amplitude of the step current response in a steady-state condition and the slope of the ramp voltage. The result showed that the capacitance could be determined using a transient waveform [8]. For large pieces of equipment, it is difficult to apply the ideal ramp voltage.

A comprehensive method to measure a small capacitance with loss is proposed in this paper. Parameters are determined using a set of transient current waveforms. As an application example, the method is used on a model circuit of an impedance between electrodes implanted into a piece of wood.

Wooden poles and cross-arms are still used in distribution systems across the world. The transient characteristic of the wooden insulator against a lightning strike is important in insulation design. One of the factors determining the characteristic is the impedance between the electrodes implanted into wood. Its equivalent circuit is important for the transients calculation of a power system.

The stray capacitance to the ground and that between phases of a circuit breaker are required for a lightning surge analysis. The practicality of the proposed method is confirmed by measurements of the stray capacitances using a miniature circuit breaker (MCB).

2. Measuring Method

2.1. Transient measurement The specimen used in this investigation is a cubic piece of wood (Japanese cypress, Hinoki) of dimensions 140 × 140 × 250 mm. Two bolts are used as electrodes with a radius r of 5 mm, distances between the

[a] Correspondence to: Diah Permata.
E-mail: etl1104@mail4.doshisha.ac.jp

Department of Electrical Engineering, Doshisha University, 1-3, Miyakodani, Tatara, Kyotanabe 610-0321, Japan

Table I. Parameters of measurement

	Distance d[mm]	Length l[mm]
Case 1	30	80
Case 2	50	80
Case 3	30	100
Case 4	50	100

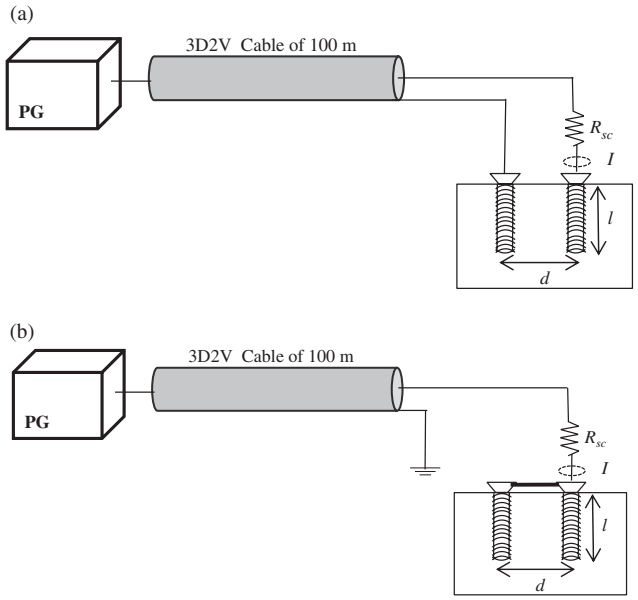

Fig. 1. Measurement setup. (a) Differential mode. (b) Common mode

electrodes d of 30 or 50 mm, and length l of 80 or 100 mm, as shown in Table I. Figure 1 illustrates the measuring circuit. A resistor R_{sc} of 10, 51, or 100 kΩ is attached to the core of the current injecting cable. The coaxial cable is 3D2V and its length is 100 m. A voltage is applied using a pulse generator (PG, Noiseken INS-4040). The transient currents are measured using a digital oscilloscope (Tektronix DPO 4104, 1 GHz) with a current probe (Tektronix CT-1).

The measurements are carried out in the differential and common modes. The first setup is for the measurement of the impedance between electrodes by connecting the electrodes to the core and sheath of the current injecting cable. The second one is for the measurement of the impedance to ground modeled by an aluminum plate. The sheath of the current injecting cable is connected to the plat, and the core to the short-circuited electrodes.

2.2. Measured result The injected currents for the cases shown in Table I are measured with three source resistances R_{sc}. The measured results are shown in Fig. 2. The vertical axis is displayed in logarithmic scale. The time constants for the differential and common modes obtained from the slope of the current waveforms in Fig. 2 are shown in Table II.

2.3. Effect of sheath surge impedance The transient measurement requires a current injecting cable. A coaxial cable should be used from a view point of high immunity to noise. Since the coaxial surge impedance ($R_{cc} = 50\Omega$ for the 3D2V cable) is connected in series to the high source resistor R_{sc}, the effect of the surge impedance is negligible. The sheath surge impedance of the current injecting cable (R_{cs}) was also neglected. In other words, the current injecting cable is neglected when a high resistance R_{sc} is connected in series to the core. However, the low value of the sheath surge impedance R_{cs} affects the transient voltage and

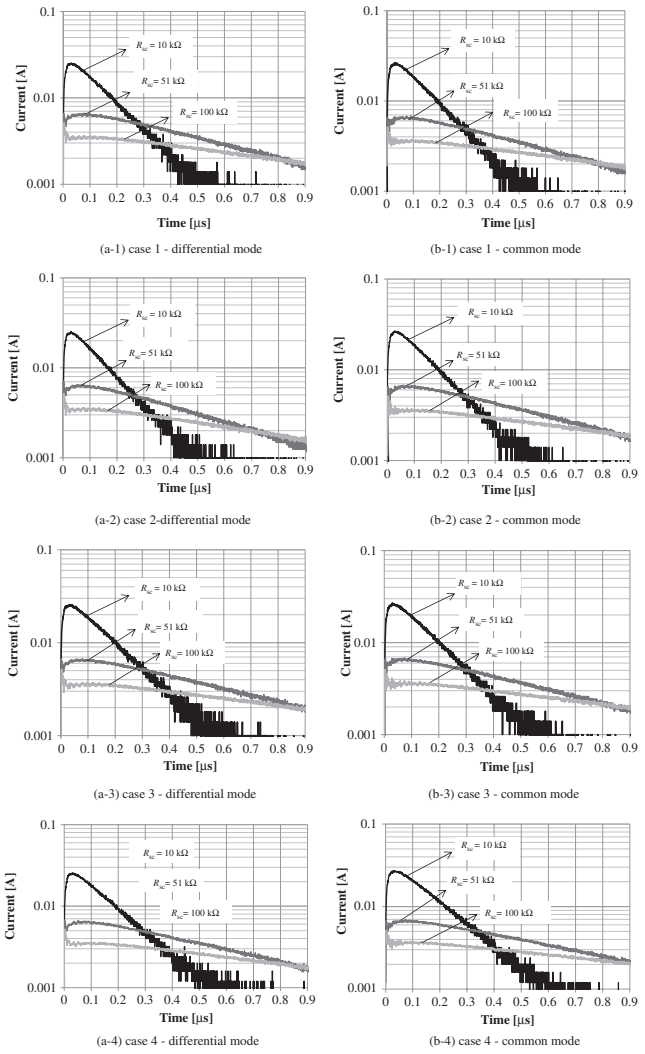

Fig. 2. Semilogarithmic plot of measured results of transient current, four cases. (a-1) case 1—differential mode, (a-2) case 2—differential mode, and (a-3) case 3—differential mode, and (a-4) case 4 differential mode. (b-1) Case 1—common mode, (b-2) case 2—common mode, (b-3) case 3—common mode, and (b-d) case 4—common mode

Table II. Measured time constants (μs)

	Differential mode			Common mode		
R_{sc} [kΩ]	10	51	100	10	51	100
Case 1	0.146	0.579	1.050	0.148	0.602	1.109
Case 2	0.133	0.505	0.915	0.143	0.616	1.169
Case 3	0.156	0.636	1.163	0.158	0.639	1.200
Case 4	0.152	0.590	1.068	0.162	0.668	1.262

current in the differential mode [5]. The sheath surge impedance is approximately given by the following equation, and becomes some hundred ohms.

$$R_{cs} = 60 \ln(2h/r_s) \quad (1)$$

where h and r_s are height and radius, respectively, of the cable.

The effect of the sheath surge impedance R_{cs} on the transient measurement is confirmed using a source circuit with two source resistors connected either to the core R'_{sc} or to the sheath R'_{ss}, as shown in Fig. 3(b). If the sum of the resistances R'_{sc} and R'_{ss} is equal to R_{sc}, i.e. $R'_{sc} + R'_{ss} = R_{sc}$, the injecting current of the circuit in Fig. 3(b)should be identical with that of the circuit shown

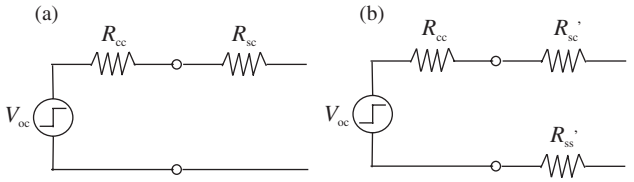

Fig. 3. Equivalent circuit of source and source resistors. (a) Single resistor. (b) Series resistors

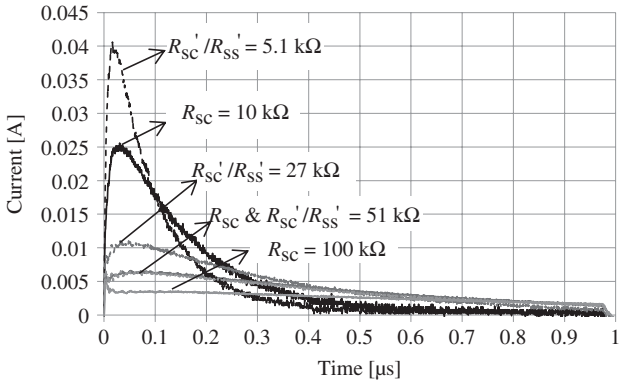

Fig. 4. Measured differential current, six cases

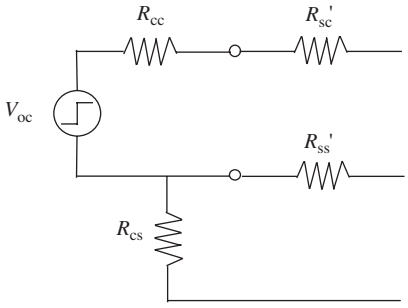

Fig. 5. Modified source circuit with sheath surge impedance R_{cs}

in Fig. 3(a). The injected current from the core flows back to the source through the resistor R'_{ss}.

The measured results of a specimen in case 4, when the series resistors R'_{sc} and R'_{ss} have the same resistance of 5.1, 27, or 51 kΩ ($\approx R_{sc}/2$), are illustrated in Fig. 4.

If the source circuit is expressed by Fig. 3(b), the current in the case $R'_{sc} = R'_{ss}$ = 51 kΩ should be almost identical to that in the case R_{sc} = 100 kΩ. However, there is 26% difference between these currents in Fig. 4. It shows that another current path exists. The sheath surge impedance R_{cs}, which was neglected in the circuit shown in Fig. 3, has to be taken into account, as will be shown later. The modified source circuit is shown in Fig. 5.

3. Result and Discussion

3.1. Equivalent circuit composition The impedances of wooden poles or wooden cross-arms have been investigated in many works. Most of them are concentrated on the preservation, reliability, and assessment of the wooden pole and leakage current against a low-frequency voltage [9–11]. However, there is no equivalent circuit expressing its high-frequency characteristic.

An equivalent circuit of electrodes implanted into a piece of wood for a high-frequency region is assumed to be a branch impedance between electrodes (Z_{el}) and ground impedances Z_g, as illustrated in Fig. 6 [4]. The ground impedance Z_g can be determined from the common mode impedance ($Z_{comm} = Z_g/2$).

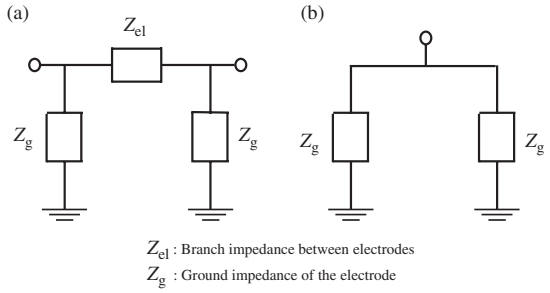

Fig. 6. Equivalent circuit for impedance between electrodes implanted into a piece of wood. (a) Total impedance. (b) Ground impedance

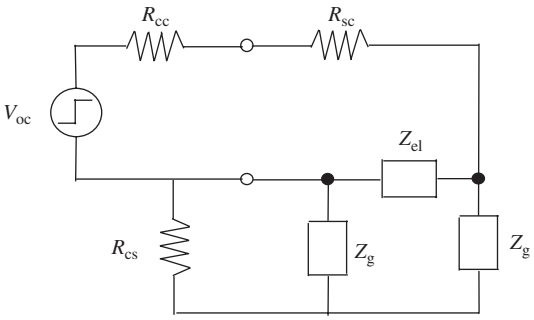

Fig. 7. Measuring system circuit in differential mode

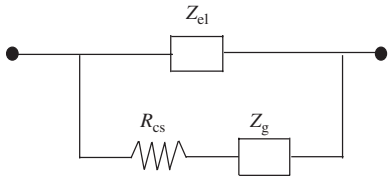

Fig. 8. Modified circuit of impedance between electrodes taking into account the effect of sheath surge impedance R_{cs}

The impedance between electrodes (Z_{el}) can be obtained from the differential mode impedance (Z_{diff}) taking into account the ground impedance Z_g and the sheath surge impedance R_{cs}.

The differential model impedance is obtained from the modified source circuit (Fig. 5) with R'_{ss} = 0 and the equivalent circuit of the impedance between electrodes (Fig. 6(a)), as shown in Fig. 7. The ground impedance Z_g is in parallel with the sheath surge impedance R_{cs}. For the 3D2V cable placed on the floor, the sheath surge impedance R_{cs} is 130 Ω, which is much smaller than the impedance Z_g. Therefore, the ground impedance Z_g connected in parallel with the sheath surge impedance can be negligible when R'_{ss} = 0. The sheath surge impedance R_{cs} becomes a series connection with the other ground impedance Z_g. The impedance of the differential mode can be approximately expressed by an equivalent circuit shown in Fig. 8. The series connected R_{cs} is also negligible because of the high impedance of the ground branch (Z_g). For the common mode test, the sheath surge impedance R_{cs} can be neglected because the sheath is directly grounded.

If the impedance can be modeled by the capacitive circuit illustrated in Fig. 9, the time constant τ for the RC circuit is expressed by (2) [12].

$$\tau = \frac{(R_{cc} + R_{sc} + R_{ac})R_{bc}}{R_{cc} + R_{sc} + R_{ac} + R_{bc}} C_{bc} \tag{2a}$$

$$\tau = \frac{(R_{cc} + R_{sc} + R_{ad})R_{bd}}{R_{cc} + R_{sc} + R_{ad} + R_{bd}} C_{bd} \tag{2b}$$

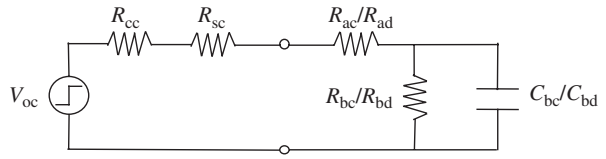

Fig. 9. Equivalent circuit of capacitive impedance

Table III. Circuit parameters of equivalent circuit

Mode	Parameter	Case 1	Case 2	Case 3	Case 4
Common	R_{ac} [kΩ]	2.75	2.20	3.21	2.97
Z_{comm} (= $Z_g/2$)	R_{bc} [MΩ]	1.23	3.86	3.29	5.14
	C_{bc} [pF]	11.7	11.7	12.0	12.5
	$\tau_{bc} = R_{bc}C_{bc}$[μs]	14.4	45.2	39.5	64.3
Differential	R_{ad} [kΩ]	3.00	3.94	2.6	3.37
Z_{diff}	R_{bd} [MΩ]	0.88	1.06	1.00	0.90
	C_{bd} [pF]	11.4	9.67	12.5	11.5
	$\tau_{bd} = R_{bd}C_{bd}$ [μs]	10.0	10.3	12.5	10.4

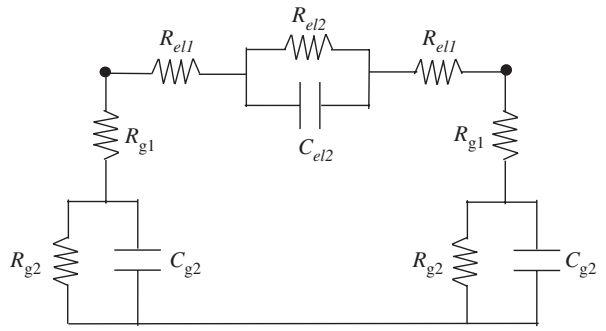

Fig. 10. Circuit of the impedance between electrodes implanted into a piece of wood

where R_{ac}, R_{bc}, and C_{bc} are for the common mode, and R_{ad}, R_{bd}, and C_{bd} are for the differential mode.

In order to obtain three unknown variables $R_{ac}/R_{ad}, R_{bc}/R_{bd}$, and C_{bc}/C_{bd}, (2) is simultaneously solved for three cases of different source resistors. The circuit parameters of the impedance in the common and differential modes are shown in Table III.

The time constants of the RC parallel circuit (τ_{bc}/τ_{bd}) shown in Table III are greater than 10 μs ($= \tau_b$). Thus, the impedance is principally determined by the resistance R_{bc}/R_{bd} in the frequency region lower than 16 kHz ($= f_b = 1/2\pi\tau_b$), and C_{bc}/C_{bd} in the region higher than the frequency f_b (middle frequency region). If the series resistance R_{ac}/R_{ad} is much smaller than R_{bc}/R_{bd}, the resistance R_{ac}/R_{ad} determines the impedance characteristic in the high-frequency region ($f \gg f_a$, $f_a = 1/2\pi\tau_a, \tau_a = R_aC_b$).

The equivalent circuit shown in Fig. 10 is composed on the basis of the following information. The series resistances R_{el1} and R_{g1} are assumed to be the contact resistances of the electrodes. The parallel circuit of R_{el2} and C_{el2} expresses the insulating resistance of the wood and the capacitance between the electrodes. The resistance and stray capacitance between the electrodes and ground are expressed by R_{g2} and C_{g2}.

Since the circuit parameters shown in Table III are determined by the low and middle frequency components, i.e. the time constants of the wave-tail shown in Table III, the uncertainty of the series resistor R_{ac}/R_{ad} should be examined. In the example of the impedance between electrodes implanted into a wood, the reliability of the parameter R_{ac}/R_{ad} ($\ll R_{bc}/R_{bd}$) can be improved using information in the high-frequency region.

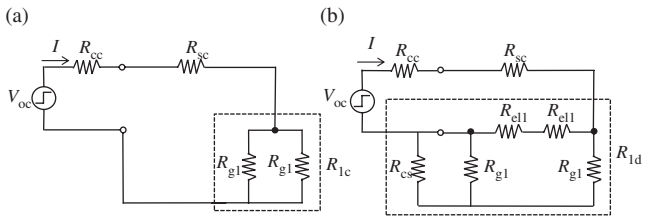

Fig. 11. Equivalent circuit in the high-frequency region. (a) Common mode. (b) Differential mode

Table IV. Estimated series resistance R_1

Mode	R_{sc} [kΩ]	Case 1	Case 2	Case 3	Case 4
Common, R_{1c} [kΩ]	10	0.97	0.93	0.91	0.84
Differential, R_{1d} [kΩ]	10	1.35	1.29	1.16	1.10

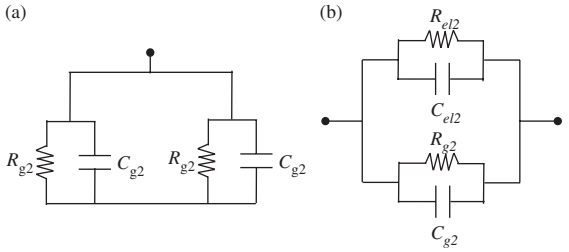

Fig. 12. Equivalent circuit in the low-frequency region. (a) Common mode. (b) Differential mode

The voltage source shown in Figs 5, 7, 8, and 9 is the open-circuit voltage V_{oc} at the end of the current injection cable. The voltage can be measured without the effect of the parasitic capacitance in the voltage probe because the internal impedance of the source determined by the coaxial-mode surge impedance of the current injection cable (50 Ω) is much lower than the input impedance of the probe.

The impedance in the high-frequency region is theoretically obtained as the ratio between the open-circuit voltage and the current injected into the circuit with some kind of time-to-frequency transformation, such as a Fourier transform. However, the noise induced into the measured results and quantization error of the waveform recorder reduce the estimation reliability of the high-frequency characteristic. The impedance in the high frequency region, i.e. the resistance in the region can be obtained from the voltage and current ratio at the wavefront in a time domain. This is a practical way compared to the sophisticated numerical time-to-frequency transformation. Since the open-circuit voltage V_{oc} is known, the series resistance can be obtained from the equivalent circuits in the high-frequency region shown in Fig. 11 and (3).

$$\frac{V_{oc}}{I} = R_{cc} + R_{sc} + R_{1c} = R_{cc} + R_{sc} + R_{g1}/2 \tag{3a}$$

$$\frac{V_{oc}}{I} = R_{cc} + R_{sc} + R_{1d} = R_{cc} + R_{sc} + 2R_{el1}//(R_{cs}//R_{g1} + R_{g1}) \tag{3b}$$

Small source resistances are preferable for an accurate estimation of the series resistance R_{g1}/R_{el1} because the resistances given in (3)have a term of the source resistances $R_{cc} + R_{sc}$. The difference between the estimated result (3a) and the source resistances ($R_{cc} + R_{sc}$) becomes a series resistance in a common mode R_{1c}. The resistance for a differential mode R_{1d} can be obtained in a

Table V. Circuit parameters of equivalent circuit

	Parameter	Case 1	Case 2	Case 3	Case 4
Z_g (= $2Z_{comm}$)	R_{g1} [kΩ]	1.94	1.86	1.82	1.68
	R_{g2} [MΩ]	2.46	7.72	6.58	10.3
	C_{g2} [pF]	5.84	5.87	6.00	6.25
Z_{el}	R_{el1} [kΩ]	1.96	1.85	1.44	1.41
	R_{el2} [MΩ]	1.36	1.23	1.16	1.00
	C_{el2}[pF]	5.56	3.80	6.51	5.25

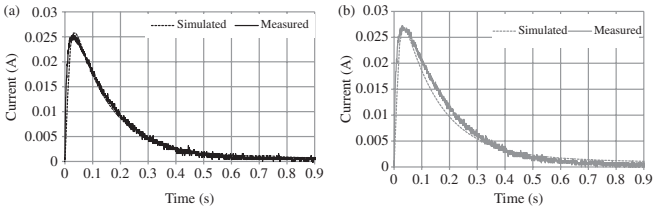

Fig. 13. Simulated results for $R_{sc} = 10$ kΩ in case 4. (a) Differential mode. (b) Common mode

similar way using (3b)as shown in Table IV. The resistances are obtained as the averaged values between the half of the wavefront time T_f of the current waveform ($T_f/2 = 8$ ns) and T_f ($8 < t < 16$ ns).

A comparison of the results R_{1c}/R_{1d} with those obtained from the wave-tail information shown in Table III as R_{ac}/R_{ad} indicates that the series resistance in the high-frequency region is smaller than that obtained from the information in the middle- and low-frequency regions.

In the middle- and low-frequency regions, the common mode impedance consists of the grounding impedances Z_g connected in parallel (Fig. 12(a)). As illustrated in Fig. 8, the differential mode impedance can be expressed by a parallel connection of Z_g and Z_{el}, as shown in Fig. 12(b).

The grounding impedance Z_g is obtained as twice the common mode impedance Z_{comm}. The equivalent circuit parameters for the impedance between the electrodes Z_{el} and the ground impedance Z_g are given by (4)using the results shown in Tables III and IV. Table V shows the circuit parameters of the equivalent circuit shown in Fig. 10. The contact resistance R_{g1} and R_{el1} are independent of the distance of the electrode d. The resistances have a decreasing tendency as the length of the electrode increases. It expresses the fact that the contact resistance is inversely proportional to the surface area. However, a clear trend cannot be observed because a stable contact between the wood and the electrode is difficult.

$$\begin{aligned} &R_{g1} = 2R_{1c};\ R_{g2} = 2R_{bc};\ C_{g2} = C_{bc}/2 \\ &R_{el1} = (R_{cs}//R_{g1} + R_{g1})R_{1d}/2[(R_{cs}//R_{g1} + R_{g1}) - R_{1d}] \\ &R_{el2} = (R_{g2}R_{bd})/(R_{g2} - R_{bd});\ C_{el2} = C_{bd} - C_{g2}) \end{aligned} \quad (4)$$

3.2. A transient simulation The transient currents flowing into the electrodes implanted into a piece of wood are simulated using Electromagnetic Transients Program (EMTP). The equivalent circuit of the impedance between electrodes shown in Fig. 10 is used to express the impedance between electrodes in the EMTP simulation.

The current injection coaxial cable 3D2V is expressed by a Semlyen's line model in the EMTP simulation taking into account its frequency dependence. A comparison between the simulated and measured results for a source resistor R_{sc} of 10 kΩ in case 4 is shown in Fig. 13. The good agreement shows that the impedance measuring method for a circuit with small capacitances has sufficient reliability.

Table VI. Capacitance between electrodes (C_{el}) obtained by measured result and theoretical calculation

	Cases		C_{el} [pF]	
	Distance d [mm]	Length l [mm]	Measured	Theoretical
Case 1	30	80	5.56	5.53
Case 2	50	80	3.80	4.05
Case 3	30	100	6.51	6.91
Case 4	50	100	5.25	5.06

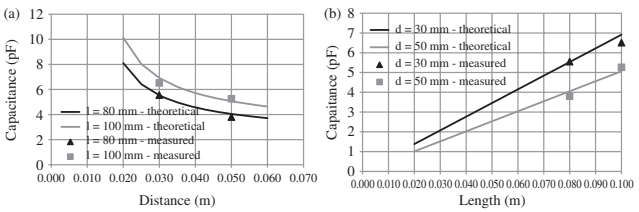

Fig. 14. Comparison between measured and theoreticalC_{el}. Function of distance. (b) Function of length

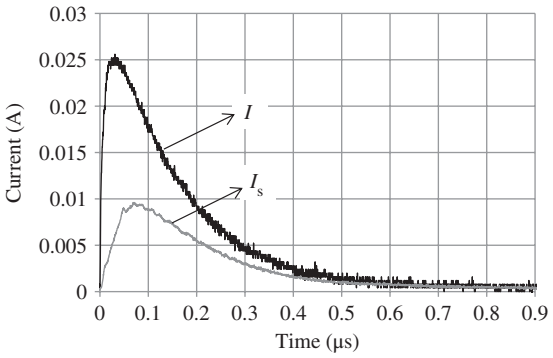

Fig. 15. Core current I and sheath current I_s in case 4

3.3. Theoretical parameters The capacitance between electrodes (C_{el}) can be approximately calculated using a theoretical equation for a parallel wire as shown in (5).

$$C = [\pi \varepsilon_0 \varepsilon_r / \ln((d - r)/r)]l \quad (5)$$

where d is the distance between the electrodes, r is the radius of the electrode, and l is the length of electrode.

The measured results of the capacitance between electrodes (C_{el}) for the cases with different distances and lengths are compared with the theoretical results in in Table VIand Fig. 14. In the theoretical calculation, the relative permittivity ε_r of dry wood is assumed to be 4 [13].

The capacitance between the electrodes (C_{el}) is inversely proportional to the logarithm of the distance d and proportional to the length l, as shown in (5). The reliability of the estimated capacitance between electrodes (C_{el}) is confirmed from Fig. 14.

3.4. Effect of sheath surge impedance The sheath surge impedance R_{cs} has a great influence on the transient measurement of the differential mode. The sheath surge impedance R_{cs} almost short circuits one of the ground impedances Z_g in the low-frequency region, as shown in Figs 7 and 8. The core current I is divided by the parallel connection of resistances Z_{el} and $R_{cs} + Z_g$.

The ratio between the current flowing through the sheath (I_s) and that into the sheath surge impedance R_{cs} (I_{cs}) can be calculated

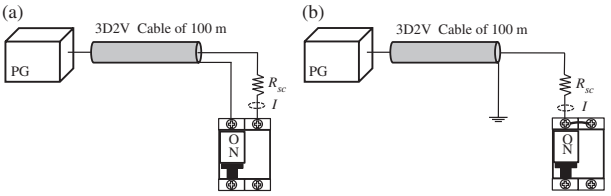

Fig. 16. Measurement setup

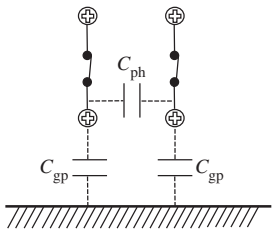

Fig. 17. Equivalent circuit of impedance in MCB

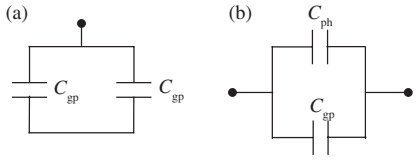

Fig. 18. Circuit of impedance in MCB. (a) Differential mode. (b) Common mode

using (6). In case 4, at the high frequency, the current ratio I_{cs}/I_s becomes 1.7, because Z_g and Z_{el} are mainly determined by the series resistances R_{g1} and $2R_{el1.}$ The theoretical ratio I/I_s becomes 2.7. A measured result of the sheath and core currents (I_s and I) is shown in Fig. 15. The ratio between their peak values I/I_s is 2.7, which is identical to the theoretical result.

$$\frac{I_{cs}}{I_s} = \frac{Z_{el}}{R_{cs} + Z_g} \approx \frac{Z_{el}}{Z_g} \tag{6a}$$

$$\frac{I}{I_s} = \frac{I_s + I_{cs}}{I_s} = 1 + \frac{Z_{el}}{R_{cs} + Z_g} \approx 1 + \frac{Z_{el}}{Z_g} \tag{6b}$$

4. Application

In this section, the proposed method is applied to an MCB. From the measured results of a stray capacitance to ground and that between phases, the applicability to a practical system and reliability of the proposed method will be discussed.

A two-pole low-voltage MCB, whose rated voltage U_e is 220 V and rated short-circuit current I_{cn} is 2.5 kA, is used in this study. The measurement setup is shown in Fig. 16. For the measurement of the capacitance between the phases, the contacts are closed ('ON') to exclude the impedance between the contacts. In the common mode test, all the terminals are short-circuited.

The equivalent circuit of the MCB impedance is similar to that in the electrodes implanted into a piece of wood. It is composed of three branches: an impedance between phases (Z_{ph}) and two impedances from the phases to ground (Z_{gp}). The model of the MCB can be expressed by capacitances, as illustrated in Fig. 17, because an MCB has a high insulating resistance, i.e. no contact resistance between the electrode and its insulator. As described in Section 3, the capacitance to ground is short-circuited by the sheath surge impedance in the differential mode measurement. The equivalent circuits in common and differential modes are shown in Fig. 18. The measured results using the proposed method are shown in Table VII.

Table VII. The capacitance of equivalent circuit using the proposed method (pF)

	MCB capacitance	With C_a
$C_{comm}(= 2C_{gp})$	15.8	←
$C_{diff}(= C_{ph} + C_{gp})$	12.1	21.9
C_{gp}	7.9	←
C_{ph}	4.2	14.0

The capacitances are measured by an impedance analyzer (Agilent 4294A) to confirm the reliability of the proposed method. The capacitances to ground and between phases measured by the instrument at the frequency 1 MHz are 8.16 and 4.02 pF, respectively. The difference between the capacitances measured by the instrument and by the proposed method is less than 5%.

A ceramic capacitor of 9.9 pF (C_a) is connected between the phases to confirm the applicability of the proposed method using a known capacitance. The capacitance in differential mode (C_{diff}) increases from 12.1 to 21.9 pF, as shown in Table VII. The increase of the capacitance between phases C_{ph} is 9.8 pF. The result shows that the proposed method estimates the capacitance within a difference of 0.1 pF.

5. Conclusion

A method to measure a small capacitance using a set of transient current waveforms has been proposed in this paper. The method enables a measurement without a voltage probe across the small capacitance. The effect of the parasitic capacitance of the voltage probe, which has a fatal disadvantage for the transient method, is removed.

The proposed method is handy because it gives the small capacitance without any time-to-frequency transformation, such as the Fourier transform. The method has high immunity against noise and quantization errors of the waveform recorder for the transient measurement. The capacitance as well as the loss resistance can be calculated from the time constant obtained from the slope of the logarithm of the injected currents in the time domain. Compared to conventional measuring methods in a steady state, the proposed method is useful for practical application in a power apparatus. However, a current injection cable is indispensable to the measurement. In this paper, the effect of the sheath surge impedance on the transient measurement, which is one of factors reducing the reliability, was investigated and a correction method proposed.

The reliability of the proposed method was confirmed by transient simulations and a theoretical analysis in the example of impedances between electrodes implanted into a piece of wood. A model circuit of the electrodes was also proposed in this paper. The model is composed of three branches: the impedance between the electrodes and two ground impedances. These elements were derived from measured results in the common and differential modes. From the results at the wavefronts, i.e. in the high-frequency components, a contact resistance between electrodes to the specimen was obtained. The resistance and capacitance in the wave-tail, i.e. in the low-frequency region, express the insulating resistance of wood and the capacitance between the electrodes.

The reliability of the proposed method was also clarified by measurements of the MCB capacitances. The method is useful for the measurement of small capacitances of a power system apparatus in practical systems as well as in laboratory tests.

References

(1) Fuhrmann H, Bengtsson T. High precision methods for online measurement of capacitance in power capacitors. *International Conference on Condition Monitoring and Diagnosis*, 2008.

(2) Kopanski JJ, Afridi MY, Chong Jiang, Ritchter CA. Test chip to evaluate measurement methods for small capacitances. *International Conference on Microelectronic Test Structure*, 2009.
(3) Natarajan S, Herman BK. Measurement of small capacitances using phase measurement. *Symposium on System Theory*, 1990.
(4) Permata D, Nagaoka N, Ametani A. A modeling method of impedance between electrodes implanted into wood . *Technical Meeting on High Voltage Engineering,* HV-13-035, 2013; 59–63.
(5) Permata D, Nagaoka N. An impedance measurement using transient waveform for a small-capacitance circuit. *Conference of IEEJ Kansai Region,* 2013.
(6) Noda T, Yokoyama S. Development of surge simulation code based on finite-difference time-domain (FDTD) approximation of Maxwell's equations. *IPST 2001*, Paper no. 010, 2001.
(7) Noda T, Tatematsu A, Yokoyama S. Improvements of an FDTD-based surge simulation code and its application to the lightning overvoltage calculation of a transmission tower. *IPST 2005*, Paper no. 138, 2005.
(8) Permata D, Nagaoka N. A modeling of an impedance between electrodes in a wood using a numerical electromagnetic analysis. *International Symposium on EMC and Transients in Infrastructures*, 2013.
(9) Wong KL, Rahmat MF. Study of leakage current distribution in wooden pole using ladder network model. *IEEE Transactions on Power Delivery* 2010; **25**(**2**):995–1000.
(10) Darveniza M, Holcombe BC, Stillman RH. An improved method for calculating the impulse strength of wood porcelain insulation. *IEEE Transactions on Power Apparatus and Systems* 1979; **98**(**6**):1909–1915.
(11) Darveniza M, Limbourn GJ, Prentice SA. Line design and electrical properties of wood. *IEEE Transactions on Power Apparatus and Systems* 1967; **86**(**11**):1344–1356.
(12) Permata D, Nagaoka N, Ametani A. A method to determine an impedance between electrodes implanted into wood using transient current waveform. *Technical Meeting on High Voltage Engineering*, HV-14-028, 2014; 57–61.
(13) Simpson W, Tenwolde A. Physical properties and moisture relations of wood. *Wood Handbook*, 1999; 3.1–3.24.

Diah Permata (Student Member) received the B.Eng. degree in Electrical Engineering from Sriwijaya University, Indonesia, in 1993, and the M.Eng. degree from Bandung Institute of Technology, Bandung, Indonesia, in 1999. She joined the Electrical Department, Lampung University, Lampung, Indonesia, as a Lecturer in 1999. Presently, she is pursuing the Ph.D. degree at the Graduate school of Science and Engineering, Doshisha University. Her scholarship is supported by the Ministry of Education, Republic of Indonesia. Her research interests include electromagnetic transients in power systems and lightning protection.

Naoto Nagaoka (Member) received the B.S., M.S., and Ph.D. degrees from Doshisha University (DU), Kyoto, in 1980, 1982, and 1993, respectively. In 1985, he joined DU, where he has been a Professor since 1999. From April 2008 to March 2010, he was the Dean of the Student Admission Center, DU. From April 2010 to March 2012, he was the Director of both the Liaison Office and the Center of Intellectual Properties, DU. Prof. Nagaoka is a Member of the Architectural Institute of Japan, The Institute of Electrical Installation Engineers of Japan, and The Institute of Electrical and Electronics Engineers.